Available online at www.sciencedirect.com
ScienceDirect
Geochimica et Cosmochimica Acta 73 (2009) 1325–1339
Geochimica et Cosmochimica Acta
www.elsevier.com/locate/gca

Tidal pumping drives nutrient and dissolved organic matter dynamics in a Gulf of Mexico subterranean estuary

Isaac R. Santos *, William C. Burnett, Thorsten Dittmar, I G.N.A. Suryaputra, Jeffrey Chanton

Department of Oceanography, Florida State University, Tallahassee, FL 32306, USA

Received 15 August 2008; accepted in revised form 19 November 2008; available online 7 December 2008

Abstract

We hypothesize that nutrient cycling in a Gulf of Mexico subterranean estuary (STE) is fueled by oxygen and labile organic matter supplied by tidal pumping of seawater into the coastal aquifer. We estimate nutrient production rates using the standard estuarine model and a non-steady-state box model, separate nutrient fluxes associated with fresh and saline submarine groundwater discharge (SGD), and estimate offshore fluxes from radium isotope distributions. The results indicate a large variability in nutrient concentrations over tidal and seasonal time scales. At high tide, nutrient concentrations in shallow beach groundwater were low as a result of dilution caused by seawater recirculation. During ebb tide, the concentrations increased until they reached a maximum just before the next high tide. The dominant form of nitrogen was dissolved organic nitrogen (DON) in freshwater, nitrate in brackish waters, and ammonium in saline waters. Dissolved organic carbon (DOC) production was two-fold higher in the summer than in the winter, while nitrate and DON production were one order of magnitude higher. Oxic remineralization and denitrification most likely explain these patterns. Even though fresh SGD accounted for only ~5% of total volumetric additions, it was an important pathway of nutrients as a result of biogeochemical inputs in the mixing zone. Fresh SGD transported ~25% of DOC and ~50% of total dissolved nitrogen inputs into the coastal ocean, with the remainder associated with a one-dimensional vertical seawater exchange process. While SGD volumetric inputs are similar seasonally, changes in the biogeochemical conditions of this coastal plain STE led to higher summertime SGD nutrient fluxes (40% higher for DOC and 60% higher for nitrogen in the summer compared to the winter). We suggest that coastal primary production and nutrient dynamics in the STE are linked.

1. INTRODUCTION

Subterranean estuaries (STE) are defined as areas where groundwater derived from recharge on land mixes with seawater that has invaded the aquifer (Moore, 1999). This term was coined to emphasize the importance of mixing and chemical reactions that occur in coastal aquifers. STE are usually characterized by longer residence times, stronger particle–water interactions, and lower dissolved oxygen than surface estuaries. The biogeochemical processes regulating the input, recycling, and removal in surface estuaries have been studied in great detail over the last few decades (Kaul and Froelich, 1984; Boynton et al., 1995; Bianchi et al., 1999; Windom et al., 1999; Pinckney et al., 2001; Valiela et al., 2002; Seitzinger et al., 2005), but their subterranean counterparts are only beginning to be explored.

Recent investigations addressed nutrient distributions in STE. Silicate and dissolved organic carbon (DOC) appeared to behave conservatively, while phosphate and nitrate had non-conservative removal in a STE from New York (Beck et al., 2007). In southern Brazil, high ammonium concentrations indicated remineralization of organic detritus (Windom and Niencheski, 2003). In two Florida environments, nutrient concentrations and ratios in coastal groundwater were strongly related to redox potential

* Corresponding author.
E-mail address: santos@ocean.fsu.edu (I.R. Santos).

0016-7037/$ - see front matter © 2008 Elsevier Ltd. All rights reserved.
doi:10.1016/j.gca.2008.11.029

(Kroeger et al., 2007; Santos et al., 2008a). Such a control was also indicated by field observations in Massachusetts and biogeochemical modeling in an idealized STE (Spiteri et al., 2008). Even in organic carbon poor conditions, the nearshore aquifer is a biogeochemically active zone, where attenuation of nitrogen can occur (Kroeger and Charette, 2008). Relevant biogeochemical and physical processes removing nutrients from subterranean estuaries include denitrification (An and Joye, 2001; Addy et al., 2005), calcium phosphate precipitation (Cable et al., 2002; Slomp and Van Cappellen, 2004), sorption of P to Fe-oxides (Charette and Sholkovitz, 2002; Charette and Sholkovitz, 2006), and submarine groundwater discharge (SGD).

Significant SGD inputs of nitrogen may be a key factor initiating and maintaining phytoplankton blooms in the coastal ocean (Hu et al., 2006). Globally, fresh groundwater discharge has been estimated to be only a few percent of the total freshwater flux to the oceans (Burnett et al., 2006). However, as dissolved species concentrations in groundwater often exceed those in surface waters, groundwater can play a significant role in dissolved species budgets even when the volume contribution is small (Santos et al., 2008b). A series of investigations demonstrated that nutrient inputs via SGD were either comparable or higher than local river inputs in a variety of environments, including salt marshes (Charette et al., 2003), coral reefs (Paytan et al., 2006), coastal lagoons (Deborde et al., 2008), and river-dominated shelves (Burnett et al., 2007). It has even been suggested that high N:P ratios in contaminated groundwaters may drive the coastal ocean towards P-limitation within the coming decades, perhaps shifting the present N-limited primary production (Slomp and Van Cappellen, 2004).

The common approach for calculating SGD-derived nutrient exports to coastal waters does not consider modifications as nutrients pass through subterranean estuaries. Simply multiplying the average nutrient concentration in continental groundwater by the fresh SGD rate will lead to accurate fluxes only for conservative species. The scientific community now recognizes the dynamic nature of SGD (Burnett et al., 2006). The view that discharge is controlled exclusively by seasonal oscillations of the water table on land has been revised. Geochemical tracer (^{222}Rn), modeling, and seepage meter results indicate that SGD may be highly variable over short time scales as a consequence of transient processes, such as tidal pumping and wave setup (Kim and Hwang, 2002; Taniguchi and Iwakawa, 2004; Robinson et al., 2007; Santos, 2008). To obtain dissolved species fluxes, temporally integrated SGD fluxes are still often multiplied by the average elemental concentration in the coastal aquifer neglecting temporal changes in groundwater biogeochemistry. Even though this may be a reasonable assumption in some cases, we suspect that endmember nutrient concentrations may be as variable as SGD rates.

In a recent investigation at the same site reported here, we described nutrient distributions in 2D transects sampled across the subterranean salinity gradient. We described qualitatively the role biogeochemical processes play in the alteration of endmember nutrient concentrations in the subsurface (Santos et al., 2008a). We hypothesized that marine forces control nutrient biogeochemistry in this STE, i.e., tidal pumping supplies oxygen and reactants in the form of particulate marine organic matter. We further hypothesized that the remineralization of these organic reactants represents a major nutrient source to shallow beach groundwaters. Our objective in the current investigation was to explore these hypotheses and to determine the factors driving nutrient biogeochemistry in a STE over short time scales. We use the standard estuarine model developed for surface estuaries and a non-steady-state box model to estimate nutrient production and consumption rates in the freshwater–seawater transition zone. We also discuss nitrogen speciation and separate the nutrient fluxes derived from fresh and saline SGD.

2. MATERIALS AND METHODS

We conducted a series of field experiments in a STE near the Florida State University Coastal and Marine Laboratory (FSUCML) in the north-eastern Gulf of Mexico (Turkey Point), a site where several previous SGD studies have been conducted. A detailed description of the study site can be found in these prior studies (Cable et al., 1996; Burnett and Dulaiova, 2003; Lambert and Burnett, 2003; Santos et al., 2008a).

In order to plan the location of the permanent monitoring wells sampled here, we used a push-point piezometer (Charette and Allen, 2006) to determine where the freshwater–seawater interface was located. Monitoring wells were then installed about 1 week before the experiments to allow the well casing to equilibrate with the surrounding sediments. In our first experiment, hereafter referred to as "vertical time series (VTS)", four wells were installed at the high tide mark at depths ranging from 0.5 to 2.5 m. This is the layer where permeable sediments occur (Fig. 1) and where groundwater is more dynamic. Samples were collected every 90 min during a tidal cycle (total of 16 h) on 30 May 2007 following standard procedures described elsewhere (Charette and Allen, 2006). Based on the results of the VTS, we designed a second experiment (hereafter referred to "as horizontal time series or HTS"). In this experiment, we sampled five wells that were horizontally distributed perpendicular to the beach face (0.5 m deep; 20 cm long screens) in the summer (August 2007) and in the winter (January 2008; Fig. 1).

Samples for inorganic nutrients, DOC and total dissolved nitrogen (TDN) analyses were collected with plastic, acid-cleaned syringes and immediately filtered through disposable 0.7 μm Whatman® GF/F syringe filters. Replicate samples were collected after discarding a small amount of filtered water. Immediately after filtering, nutrient samples were kept on ice in the dark until they could be frozen (within a few hours of collection). Nutrient analysis was conducted within 1 week of sampling using standard colorimetric methods (Grasshoff et al., 1999). Analytical errors, based on the standard deviations of triplicate samples, were lower than 6% for nitrate, phosphate, and silicate and 7% for ammonium. DOC and total dissolved nitrogen (TDN) samples were acidified to pH 2 with HCl, sealed into glass ampoules in the field, and analyzed with a Shimadzu

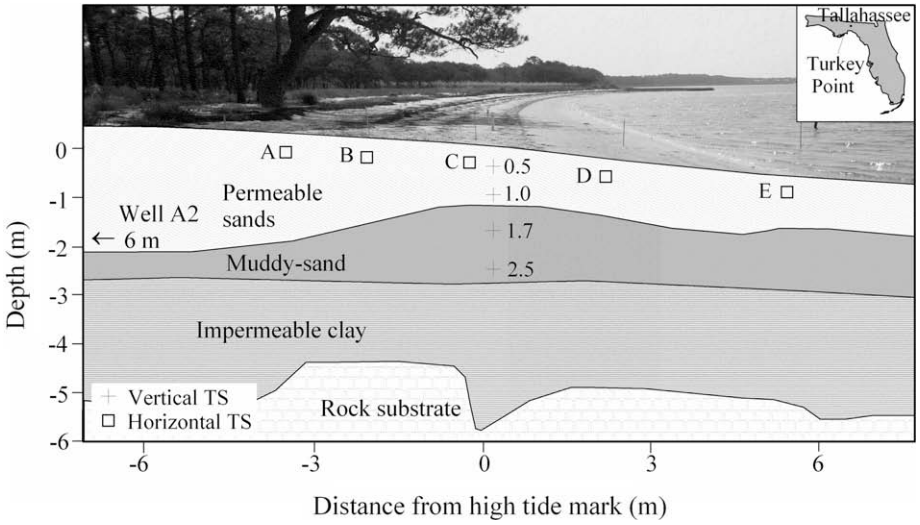

Fig. 1. Location of the wells sampled for the vertical (crosses) and horizontal (squares) time series experiments. The image was taken at low tide.

TOC-V_{CPH} total organic carbon analyzer equipped with a TNM-1 total nitrogen measuring unit. Errors for DOC and TDN were within 5%. Dissolved organic nitrogen (DON) was calculated as the difference between the TDN and the sum of NH_4^+ and NO_3^-.

Groundwater level, temperature, and conductivity were monitored (10-min intervals) using CTD Divers (Van Essen instruments®). The CTD divers were not deployed in the same wells used for sampling nutrients, but rather in dedicated shore-parallel wells installed about 1 m away from the

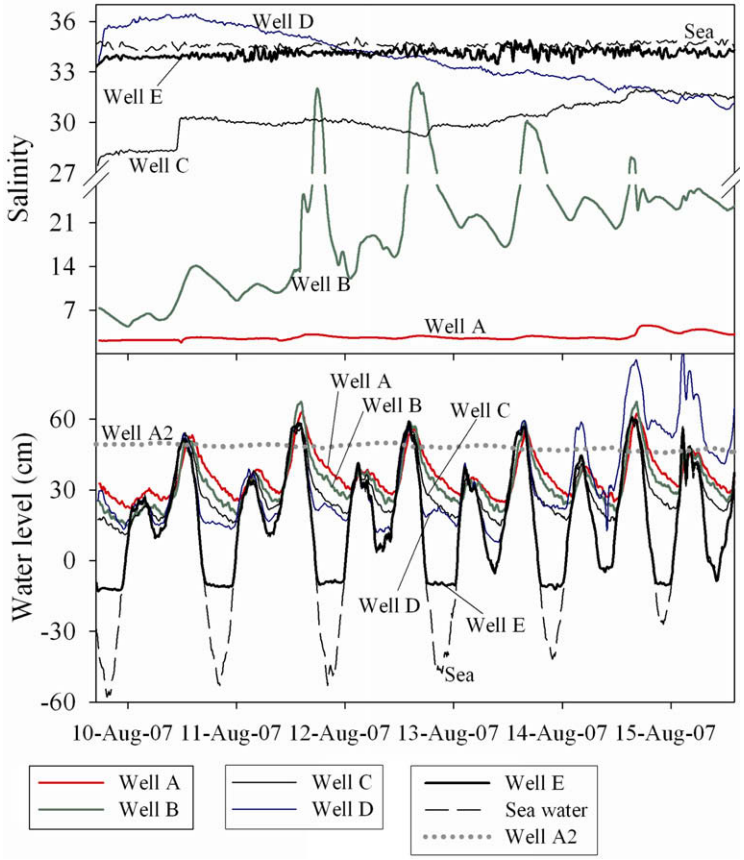

Fig. 2. A week-long time series of water level and salinity for the wells A through E, A2, and seawater. The water levels are reported relative to the same vertical datum (NAVD 1988).

nutrient wells. This ensured no disturbances in the well level recording during pumping for nutrient sampling.

During our VTS experiment, we also performed a shore-normal surface seawater transect extending 5 km offshore. Seawater DOC, TDN, and short-lived radium isotopes (^{224}Ra and ^{223}Ra) were measured along this transect. Radium sampling was carried out by passing large volumes of water (60 L) through a "Mn fiber" adsorber, which quantitatively removes radium from water. Activities of ^{223}Ra ($t_{1/2} = 11.4$ days) and ^{224}Ra ($t_{1/2} = 3.66$ days) were then measured on a delayed coincidence counter (Moore and Arnold, 1996).

3. RESULTS AND DISCUSSION

3.1. Water table and salinity temporal dynamics

We observed strong changes in the salinity of shallow beach groundwaters over short time scales and density inversions, i.e., the occurrence of denser saline water overlying less dense freshwater as a result of seawater recharging the STE. While the salinity of the shallowest well (0.5 m) from the VTS ranged from 24 to 34, the wells deeper than 1 m were fresher and varied over narrower ranges (~2 salinity units). Due to high sediment permeability, the beach groundwater level responded immediately to the increasing tide (Fig. 2). During the ebb tide, the groundwater table decreased quickly during the first couple of hours and slower later. While the tidal range of Well A (furthest inland) is just about 30% of the total oceanic tides, Well E (most offshore) varies as much as 70%. Well A2, located 15 m onshore from the high tide mark, was always completely fresh and its level did not follow tidal fluctuations. We use the continuous CTD diver observations to model groundwater velocities and estimate the residence time of the STE. The horizontal advection term (ω) was modeled following Darcy's Law in a manner similar to that described elsewhere (Taniguchi and Iwakawa, 2004):

$$\omega = k_h \frac{di}{dh} \quad (1)$$

where k_h is the local hydraulic conductivity of the sediments and di/dh is the slope of the potentiometric surface or the ratio between the vertical head (di) and the horizontal distance between two consecutive wells (dh). By multiplying horizontal velocities (ω; m day^{-1}) by the thickness of the shallow aquifer, one can obtain volumetric water fluxes (m^3 m^{-1} day^{-1} or m^3 day^{-1}/m of shoreline).

Hydraulic conductivities at this STE reached 25 m day^{-1} in the upper meter of the aquifer and approached zero at 3 m (Li, personal communication). The average gradients during the Horizontal TS in the summer and in the winter were 0.022 and 0.016, respectively. Due to low precipitation in the months preceding sampling (Table 1), these values were lower than the typical gradients observed in this area (~0.03), resulting in calculated horizontal groundwater velocities of 0.55 and 0.40 m day^{-1} for the upper meter of the aquifer. In a manner similar to that used for many surface estuaries, we define the residence time as the time required for groundwater to be transported from the fresh to the saline portion of the STE. For a mixing zone that was not longer than 7 m in the summer and 8 m in the winter, we estimate maximum estuarine residence times of 13 and 20 days, respectively (Table 1), for the upper meter of the aquifer.

Table 1
Summary of some key environmental conditions during the three sampling campaigns.

	Vertical TS 30 May 2007	Horizontal TS 10 August 2007	Horizontal TS 6 January 2008
Groundwater level* (cm)	53	49	50
Rainfall** (mm)	2	40	21
Groundwater temperature (°C)	22	25	23
Seawater temperature (°C)	27	32	16
STE residence time (days)	—	12.7	20.0
Tidal range (m)	1.02	0.99	0.94
Rn in seawater*** (dpm/L)	4.4	6.5	—
^{222}Rn-derived SGD*** (cm/day)	8.8	15.5	—

* Referenced to 1988 NAVD for well A2, located ~15 m from the mean high tide line.
** Total precipitation in the month preceding sampling.
*** Average during the period of nutrient sampling.

As an impermeable mud layer occurs at about 3 m (Fig. 1), we assumed that the diffuse fresh groundwater seepage originated only from this upper permeable aquifer. By applying Darcy's Law and using different hydraulic conductivities for the different permeable sediment layers (25 m day^{-1} for the upper meter of the aquifer; 5 m day^{-1} between 1 and 2 m; and 1 m day^{-1} between 2 and 3 m), we estimate that the volumetric addition of fresh SGD was 0.7 and 0.5 m^3 m^{-1} day^{-1} in the summer and winter, respectively. About 80% of this fresh SGD derived from the upper meter of the aquifer. Other investigators also demonstrate that shallow coastal sediments are more physically and biologically active, and experience higher rates of irrigation than deeper sediments (Huettel and Rusch, 2000; Ullman et al., 2003; Martin et al., 2006).

The Darcy's Law approach compares well with the values estimated from a variable-density hydrological model, which estimated fresh SGD rates ranging from 0.2 to 2.2 m^3 m^{-1} day^{-1} for the same area (Li, personal communication). Comparing to the total ^{222}Rn-derived SGD rates estimated from 2 years of continuous observations (average of 22 m^3 m^{-1} day^{-1}), Darcy's Law-derived fresh SGD represents only a minor fraction (~5%) of the total volumetric additions. A simple salinity mixing model in seepage meter water, described in a companion paper (Santos, 2008), confirmed the small contribution of fresh SGD, indicating that marine drivers (likely tidal pumping) control SGD rates at this site.

3.2. Nutrient variability and mixing diagrams

Nutrient concentrations were highly variable over tidal time scales in the upper meter of the aquifer, as illustrated

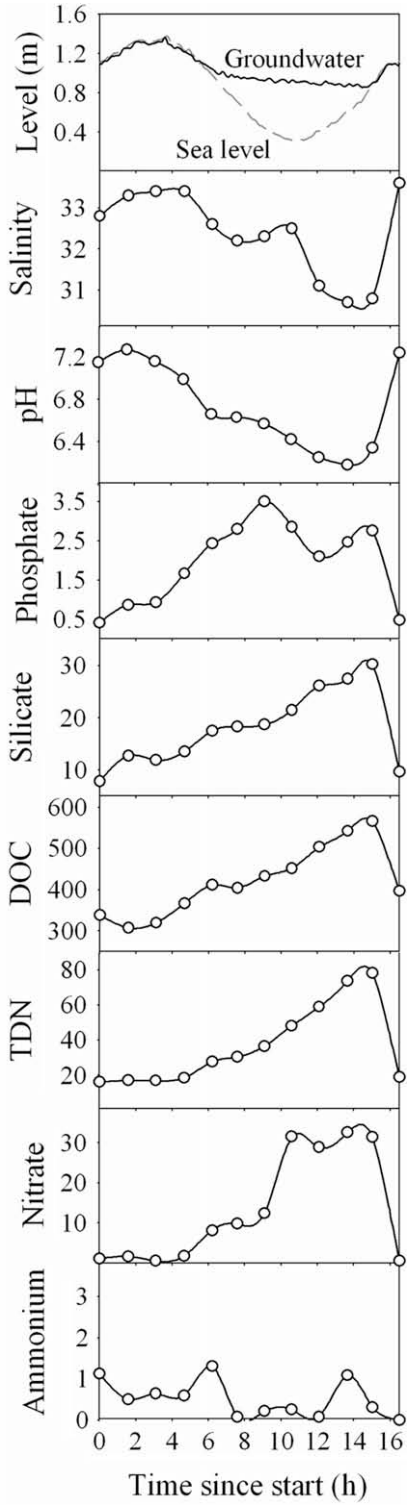

Fig. 3. Temporal variability of nutrients and associated variables in the vertical TS well 0.5 m. Nutrient concentrations in μmol L^{-1}.

in Fig. 3. At high tide, the concentrations were very low as a result of dilution caused by seawater recirculation. During ebb tide, the concentrations increased. At the beginning of flood tide, concentrations further increased until they reached a maximum just before the high tide. Similar patterns were observed for all nutrients, but nitrate had the broadest range. For example, it ranged from 0 to 35 μmol L^{-1} in the 0.5 m deep well (VTS). The concentrations in the deeper layers had a more narrow range, as can be inferred from Fig. 4. Redox potential values during the VTS experiment had no clear temporal patterns and decreased from about 50 mV at the 0.5 m well to −150 mV at the 2.5-m deep well. All the nutrients had significant negative correlations ($n = 12$; $p < 0.01$) with salinity for the 0.5 m well (see insets in Fig. 4). The VTS wells 1, 1.7, and 2.5 m did not have any noticeable short-term temporal trends and had no nutrient–salinity correlations. The zero salinity intercepts on these plots suggest that the nutrient concentrations in the fresh groundwater source are much higher than the ones observed in the deep samples. The fact that samples from the deep wells plotted off the trend (especially nitrogen species) offers evidence that vertical mixing in this aquifer is reduced compared to horizontal fluxes.

To gain insights into why the zero salinity intercept was so high in the 0.5 m well from the VTS, we conducted experiments that focused only on the upper meter of the aquifer (Horizontal TS). Interestingly, the five HTS wells were anoxic or sub-oxic both in the winter and the summer, indicating high microbial activities at this area. In the summer, we found maximum redox potential values of −76 mV. In the winter, we did not measure redox potential, but dissolved oxygen values also indicate a sub-oxic environment (average of 2.6 mg L^{-1}). No discernible spatial or temporal trends were observed for redox potential or oxygen during the HTS experiments. The results of the HTS also indicated that nutrient concentrations (except for silicate) in brackish waters cannot be explained by conservative mixing between the freshwater upgradient and the saline water downgradient (Fig. 5). Nitrate and TDN in brackish waters were much higher than the theoretical conservative dilution line, and DOC was slightly higher. Silicate behaved conservatively in the three experiments. Ammonium in the summer and phosphate both in the summer and in the winter exhibited significant scatter when plotted against salinity, most likely as a result of the complexity of the uptake, regeneration, and nitrification reactions occurring here.

In the summer, the brackish water wells had strong temporal variability. For example, nitrate ranged from 0 to 700 μmol L^{-1} over only 12 h in well C. In the winter, the temporal variability was smaller, but clear spatial patterns were observed, as can be inferred from Fig. 6. Ammonium reached 50 μmol L^{-1} in well A, approached zero in wells B–D and increased again to about 20 μmol L^{-1} in well E. Concurrently, nitrate approached zero in Well A and reached 50 μmol L^{-1} in wells B–D (Fig. 6). This suggests a complete transformation of ammonium into nitrate. The fact that nitrate approached zero again in well E and ammonium did not increase to its original level indicates nitrogen losses between wells D and E. These changes lead to extremely variable proportions of the nitrogen species over small spatial and temporal scales. While DON was ubiquitous, nitrate and ammonium approached zero in many samples (Fig. 7). The fresh and saline portions of the STE were dominated either by DON or ammonium.

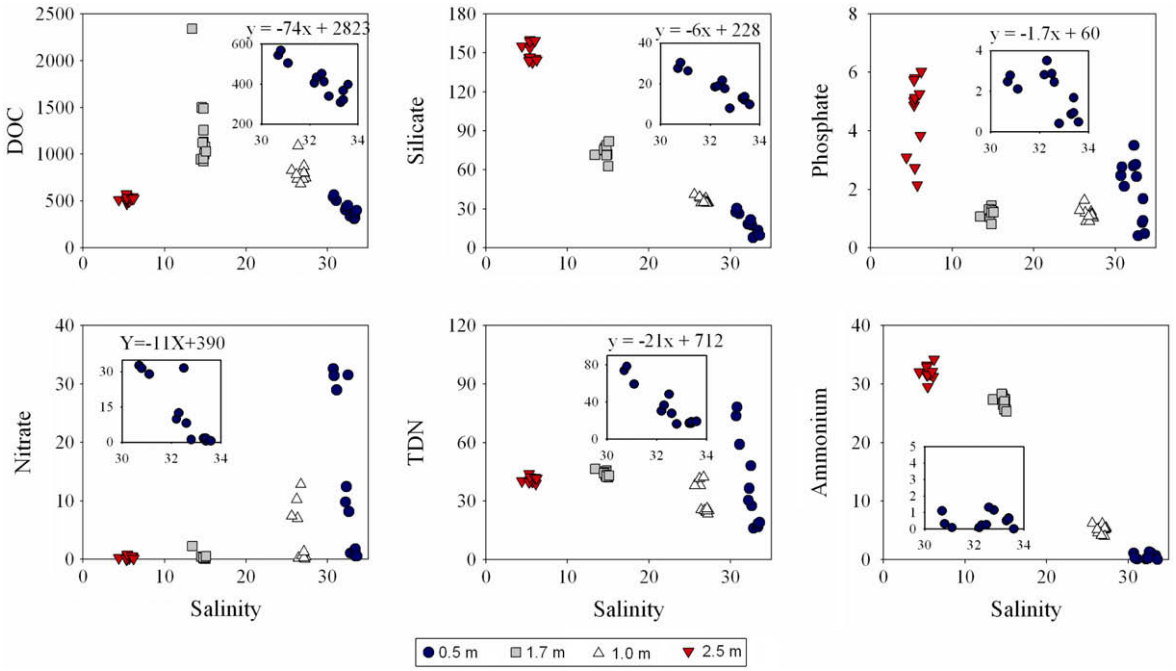

Fig. 4. Nutrient–salinity relationships for the vertical TS wells. The blown up and the equations show the samples from the VTS 0.5 m well. Nutrient concentrations in μmol L^{-1}.

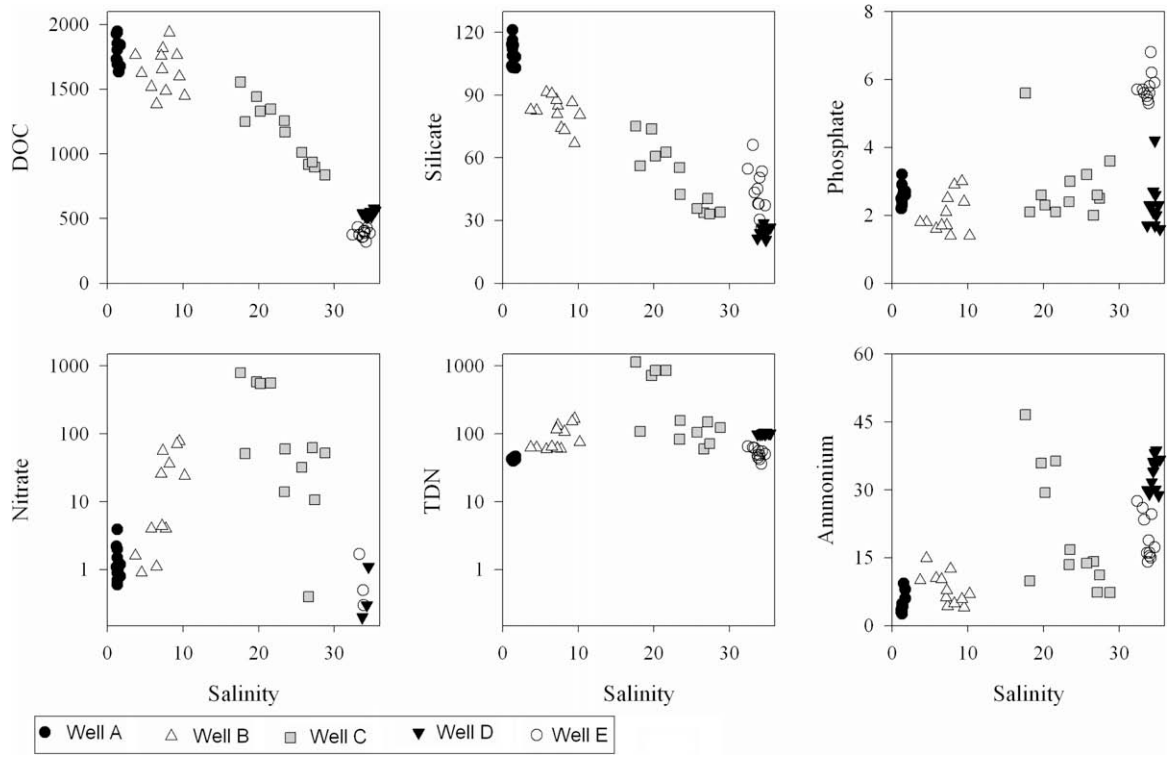

Fig. 5. Nutrient–salinity relationships for the horizontal TS wells in the summer (August 2007). Nutrient concentrations in μmol L^{-1}.

The brackish waters, in turn, were often dominated by nitrate. This illustrates the complexity of the biogeochemical processes taking place and points to the need for additional research about nitrogen speciation in SGD.

3.3. Nutrient production rates

The curvatures of some of the nutrient–salinity scatter plots offer evidence of nutrient production in the brackish

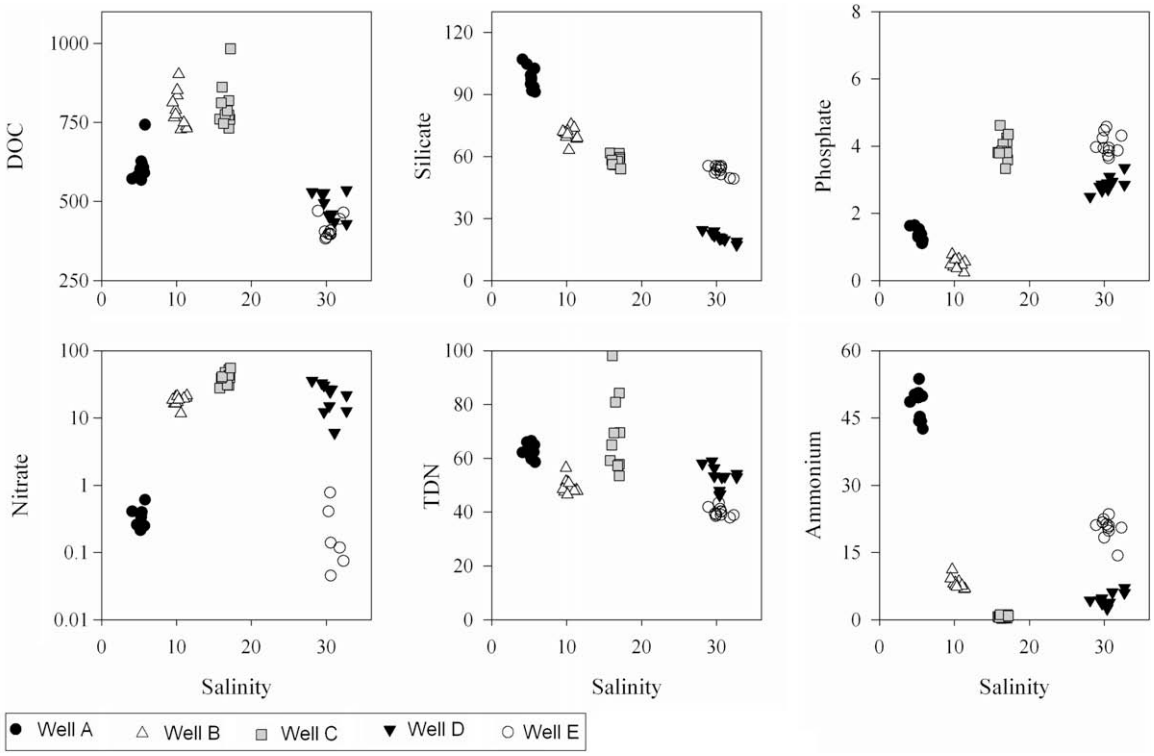

Fig. 6. Nutrient–salinity relationships for the horizontal TS wells in the winter (January 2008). Nutrient concentrations in μmol L^{-1}.

shallow groundwaters of this STE. We consider two independent models to quantify nutrient production (or consumption) rates in the shallow aquifer using the observations of the horizontal TS experiment: (1) the standard estuarine model based on the integrated areas of nutrient–salinity curvatures compared to the theoretical conservative mixing; and (2) a non-steady-state box model based on the rate of nutrient change across the beach profile.

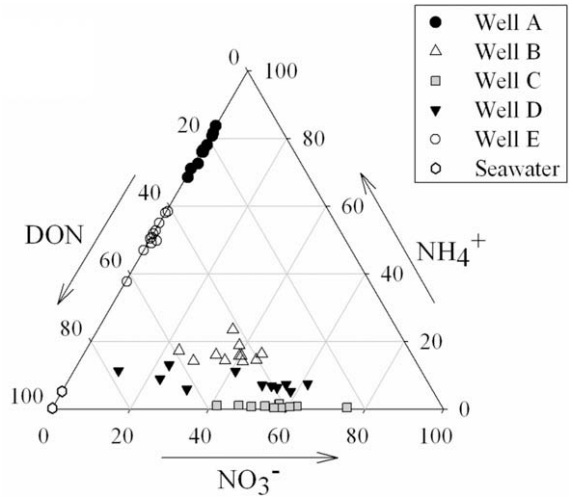

Fig. 7. Ternary diagram illustrating the percentage of the different nitrogen species for the horizontal TS in the winter.

3.3.1. The standard estuarine model

Nutrient distributions in surface estuaries have been modeled as linear mixing (conservative), first-order removal (nutrient consumption or uptake by particles), and parabolic input (nutrient production or release from particles) (Boyle et al., 1974; Kaul and Froelich, 1984). In such an analysis, salinity can be used as the conservative property and the composition of the two mixing endmembers is assumed to be constant. In our previous investigations at this site (Santos et al., 2008a), we performed 2D-transect sampling covering different sediment layers and found no simple relationship between nutrient concentrations and salinity because of vertical sediment heterogeneity in the STE. However, because the samples from the horizontal TS experiments were collected from the same sediment layer (Fig. 1), the effects of sediment heterogeneity are reduced and unambiguous nutrient–salinity relationships are now observed. We can thus model overall biogeochemical reaction rates (R; Fig. 8a) using the equations that best describe the nutrient–salinity relationships:

$$R = \frac{1}{t}\int_{S=0}^{S=35}(C_r - C_c)dS \qquad (2)$$

where t is the residence time of the mixing zone and S is salinity. We integrate the area under (or above) the equation that best fits the observed nutrient–salinity relationship (C_r) and subtract the area that can be explained by conservative mixing (C_c). A positive R represents production, while a negative R represents consumption. Sources and drivers of R cannot be evaluated from this analysis.

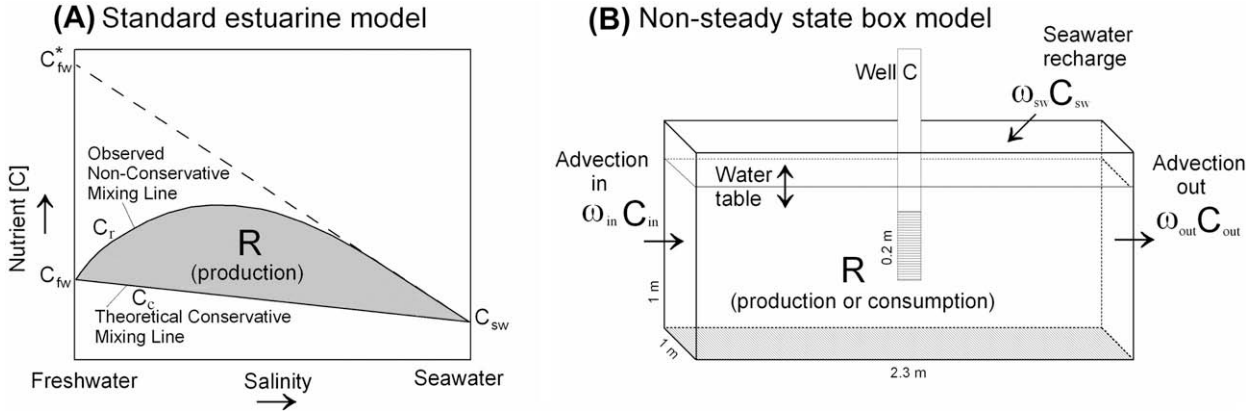

Fig. 8. Schematic diagrams illustrating the models applied for estimating biogeochemical reactions rates. (A) Standard estuarine model; and (B) non-steady-state box model. See Section 3.3 for a description of the terms used here.

Table 2 shows the equation coefficients that represent the curvatures of the nutrient–salinity relationships and the production rates derived from Eq. (2). Phosphate in both the winter and in the summer and ammonium in the summer did not correlate with salinity and thus were not included in this analysis. Our estimated nitrogen production rates ($NH_4^+ + NO_3^- + DON$) were 2–3 orders of magnitude higher than values observed in sediments of the South Atlantic Bight (0.2–1.4 mmol N m^{-2} day^{-1}), where remineralization accounts for a large fraction of new N inputs (Rao et al., 2007). We emphasize, however, that while continental shelves are ~100 km wide, the STE investigated here is only about 10 m wide. Therefore, if we scale up these results and express them in terms of unit length of shoreline, the STE nitrogen production rates would be 1–2 orders of magnitude lower than the shelf-wide production. In the summer, DOC production was two-fold higher, and nitrate and DON production were one order of magnitude higher. This suggests that higher summer phytoplankton production in this area (Mortazavi et al., 2000) is an important driver of nutrient dynamics in the STE.

3.3.2. Non-steady-state box model

While the standard estuarine model provides overall reaction rates, a one-dimensional advection–diffusion model can be adapted to estimate biogeochemical reaction rates along specific segments of the STE and thus provide insights into nutrient cycling in beach groundwaters:

$$\frac{\partial C}{\partial t} = D_s \frac{\partial^2 C}{\partial x^2} + \omega \frac{\partial C}{\partial x} + R \quad (3)$$

where $\partial C/\partial t$ is the change in nutrient concentration over time; D_s is the wet sediment diffusion coefficient, ω is the advection rate, and R is the reaction rate, e.g., a zero order nutrient production or consumption term. While horizontal advection rates are in the order of 10^{-6} m s^{-1} for the typical hydraulic gradients observed on the beach, diffusion coefficients are in the order of 10^{-9} m^2 s^{-1} (Fetter, 2001). For ω:D_s ratios >> 1 (Péclet number), transport through sediments becomes essentially advective and molecular diffusion becomes negligible, as has been demonstrated for dissolved species budgets in a number of nearby (Cable et al., 1996; Lambert and Burnett, 2003) and other permeable sediment sites (Martin et al., 2007; Rouxel et al., 2008).

Table 2
Equations describing nutrient–salinity relationships shown in Figs. 5 and 6, where nutrient concentrations [C] equal $aS^2 + bS + c$. Uncertainties represent standard errors of the respective coefficients. The "r" column shows the correlation coefficients (only correlations at $p < 0.01$ were included here). The integrated reaction rate (R) was calculated from Eq. (2) (Fig. 8a) assuming a 1-m deep layer. To convert reaction rates (mmol m^{-2} day^{-1}) into rates per unit length of shoreline (mmol m^{-1} day^{-1}), one can simply multiply the values shown by the width of the STE (~10 m).

	Behavior	Non-conserv. equation coefficients			r	R (mmol m^{-2} day^{-1})
		a	b	c		
Summer						
DOC	Production	−1.0 ± 0.2	−3.7 ± 5.8	1771 ± 39	0.98	984 ± 267
Silicate	Conservative	0.0 ± 0.0	−2.4 ± 0.1	107 ± 2	0.97	0 ± 0
Nitrate	Production	−0.9 ± 0.2	33.7 ± 6.5	−81 ± 39	0.58	364 ± 308
Ammonium	Unclear	—	—	—	—	—
DON	Production	−0.3 ± 0.1	11.2 ± 2.2	13.9 ± 13.8	0.55	202 ± 16
Winter						
DOC	Production	−1.5 ± 0.1	48.1 ± 5.3	422 ± 39	0.92	516 ± 79
Silicate	Conservative	0.0 ± 0.0	−2.9 ± 0.1	108 ± 2	0.98	0 ± 0
Nitrate	Production	−0.2 ± 0.0	7.6 ± 0.8	−35.3 ± 5.8	0.80	79 ± 6
Ammonium	Removal	0.2 ± 0.0	−7.9 ± 0.6	79.1 ± 4.7	0.91	−40 ± 4
DON	Production	−0.1 ± 0.0	3.0 ± 0.5	0.8 ± 4.0	0.64	16 ± 36

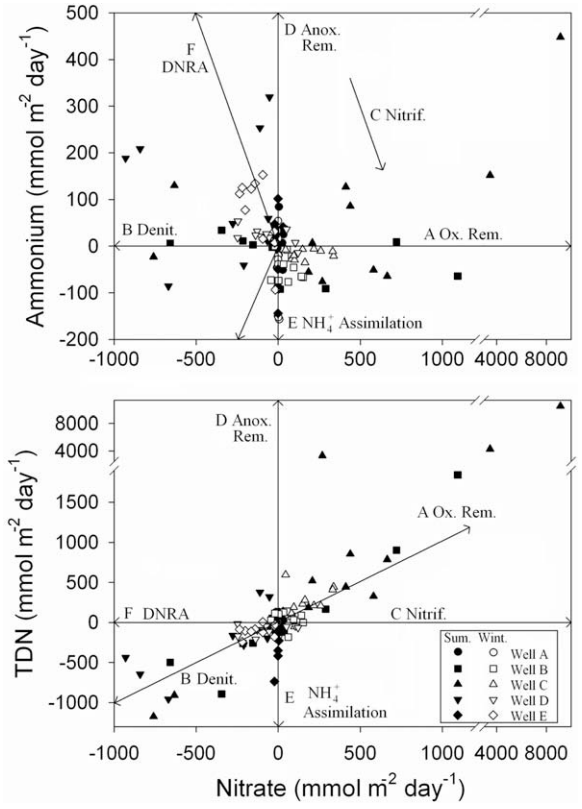

Fig. 9. Relationships between the production (positive values) or consumption (negative) of nitrate, total nitrogen, and ammonium based on the non-steady-state box model. The biogeochemical reactions likely leading to this behavior are noted: (A) oxic remineralization; (B) denitrification; (C) nitrification; (D) anoxic remineralization; (E) ammonium assimilation; (F) DNRA; (G) anammox. Diagram based on Hays and Ullman (2007).

Using the change in nutrient concentration over time as a measure of the total flux into or out of a box in the shallow aquifer, Eq. (3) can be simplified as follows:

$$\frac{\Delta C}{\Delta t} = \omega_{in} C_{in} - \omega_{out} C_{out} + \omega_{sw} C_{sw} + R \quad (4)$$

where $\Delta C/\Delta t$ is the rate of change of the nutrient concentrations; $\omega_{in} C_{in}$ is the advective nutrient input from upstream; $\omega_{out} C_{out}$ is the advective output downstream; and $\omega_{sw} C_{sw}$ is the input from seawater recharge. We calculate ω_{sw} by considering the volume of seawater infiltration required to explain the increase in salinity within a certain well. Had we not included this term, decreasing nutrient concentrations caused simply by seawater dilution would be incorrectly interpreted as nutrient consumption. The boundaries of the boxes were defined as the mid-point of two consecutive Horizontal TS wells, as illustrated in Fig. 8b.

We assume that the reaction rates derived from Eq. (4) integrate the upper 1 m of the shallow aquifer, from which 80% of fresh SGD is derived (Santos, 2008). Thus, if one assumes that these estimates are integrating the entire permeable layer (3-m deep; Fig. 1), our nutrient production rates (Fig. 9) would be underestimated by no more than a factor of 3. We also assume that vertical groundwater upwelling is small compared to horizontal groundwater transport downgradient. This assumption is supported by the absence of vertical pressure heads in wells deployed at the high tide mark at 1 and 2.5 m (data not shown). In addition, vertical conductivities at this site are 1–2 order of magnitudes lower than the horizontal conductivities (Smith and Zawadzki, 2003). Finally, modeling investigations demonstrated small vertical advection compared to horizontal fluxes at other sandy beaches (Uchiyama et al., 2000).

The results of our non-steady-state box model suggest active nitrogen cycling at this site. The values derived from the standard estuarine model (Table 2) fall within the range of the values derived from the box model (Fig. 9). Following an approach described elsewhere (Hays and Ullman, 2007), we consider seven reactions that may drive nitrogen dynamics: (a) oxic remineralization, (b) denitrification, (c) nitrification, (d) anoxic remineralization perhaps driven by sulfate respiration, (e) NH_4^+ assimilation by fine-grained sediments or bacteria, (f) DNRA (dissimilatory nitrate reduction to ammonium), and (g) anammox. Our results point to a complex combination of biogeochemical processes that are likely to occur simultaneously. The non-steady-state box model indicates that oxic remineralization would most likely explain the distribution patterns and nitrogen production observed (Fig. 9). A major problem of our non-steady-state box model is that we cannot unambiguously differentiate between reactions. For example, a combination of anoxic remineralization and nitrification could also result in the patterns assumed to represent oxic remineralization. However, the tidally-driven input of organic matter and oxygen and the labile nature of marine DOC support oxic remineralization as the major reaction controlling nitrogen production.

Denitrification and anammox are the two reactions that can permanently remove nitrogen from this system and may be responsible for the consumption between wells C and D. Anammox may occur along with nitrification, as NH_4^+ and NO_3^- co-occur in some samples collected from well C. It is very difficult to speculate about DNRA, as the samples plotting near the DNRA line (Fig. 9) may also represent a combination of anoxic remineralization and denitrification. The upper part of the STE located between wells A and C and above the high tide mark is the preferential area for nitrogen production, while the lower part of the estuary (between wells C and E) is the site of nitrogen consumption. Even though the dominant modes of nitrogen cycling at this area appear to be similar over the year, the reactions appeared more intense and varied over a wider range in the summer, probably as a result of higher organic matter content and faster flushing (e.g., lower residence time).

3.4. Fresh and saline SGD nutrient fluxes

We use our horizontal TS results in combinations with groundwater fluxes to estimate nutrient fluxes to the coastal ocean. The current definition of SGD includes both fresh SGD (the terrestrial component) and recirculated saline SGD (the marine component) (Burnett et al., 2003). Recent investigations at this site provided evidence that recirculat-

ed seawater driven primarily by tidal pumping accounts for ~95% of total SGD fluxes (Li, personal communication; Santos, 2008). Average total groundwater advection rates derived from ^{222}Rn modeling (see details in Burnett and Dulaiova, 2003) in August 2007 were 15.2 cm day^{-1} (Table 1). The average for January 2007 was 17.2 cm day^{-1}. We thus use these values as representative of SGD fluxes in January 2008, when no ^{222}Rn data are available and we carried out the second HTS experiment. Assuming a 200-m wide seepage face as determined from seepage meter deployments at the same site (Taniguchi et al., 2003), these ^{222}Rn-derived total SGD rates convert into 31.0 and 34.4 m^3 m^{-1} day^{-1}, respectively, values much higher than the fresh SGD derived from Darcy's Law (0.7 and 0.5 m^3 m^{-1} day^{-1}).

Because of steep biogeochemical gradients in the STE, determining endmember nutrient concentrations for flux calculations is not straight-forward (Charette and Sholkovitz, 2006; Beck et al., 2007). We assume that the saline SGD nutrient endmember is equal to the nutrient concentrations in saline groundwater minus the seawater concentration. By doing so, we estimate the net saline SGD input and account for nutrients added to seawater only due to saline water advective exchange. We elected to use the average concentrations in well E, as it is entirely saline and no major tidal-related biogeochemical changes were observed in this well. Nutrient concentrations deviated only ~15% from the average within a tidal cycle in well E, while concentrations ranged over one order of magnitude in the brackish water wells B and C. In addition, observations across an offshore groundwater transect (50 cm deep, data not shown) indicate that Well E concentrations are comparable to the values observed along the 200 m seepage face where saline exchange dominates, supporting our saline SGD endmember choice.

For estimating the fresh SGD endmember, we use the effective freshwater concentration (C^*_{fw} – Fig. 8a), a concept widely applied in surface estuaries (Kaul and Froelich, 1984; Davies and Eyre, 2005). This term was also recently used to estimate uranium fluxes in a STE (Charette and Sholkovitz, 2006), but neglected in most previous SGD investigations. In short, we extrapolate the trend of the nutrient concentrations in the brackish/saline waters back to the zero salinity intercept, yielding C^*_{fw} after production or consumption within the estuarine mixing zone. Phosphate was not included in this analysis because it showed no significant correlations with salinity. As a result of nutrient production in the STE, the fresh SGD effective endmembers are much higher than the saline endmembers for DOC, nitrate, and DON (Table 3). The ammonium endmember is negative due to consumption in the STE. Therefore, mixing in the subterranean estuary is a sink rather than a source of ammonium at this site. Had we not estimated the C^*_{fw}, freshwater nutrient endmembers would have been much lower, yielding vastly underestimated SGD nutrient fluxes. For example, nitrate, ammonium, and DON concentrations in fresh groundwater onshore of this site are 0, 18, and 14 μmol L^{-1}, respectively, values that would lead to fresh SGD–TDN inputs at least five-fold lower than the ones calculated here (Table 3).

Our flux calculations indicate that even though marine drivers dominate total SGD volumetric additions, fresh SGD is an important pathway of nutrients as a result of biogeochemical inputs across the mixing zone. This pathway accounted for 16–34% of DOC and ~50% of total nitrogen inputs. The remaining fluxes ("saline SGD" in Table 3) were associated with a one-dimensional vertical seawater circulation in and out of the aquifer along a conservatively estimated 200 m wide seepage face. All the nitrate inputs were associated with fresh SGD, while all the net ammonium input were related to seawater recirculation. Fluxes in the summer were about 40% higher for DOC and 60% higher for TDN compared to the winter. Hence, though SGD volumetric inputs are similar seasonally (Santos et al., 2009), changes in the biogeochemical conditions of the STE lead to higher nutrient fluxes in the summer. We emphasize that fresh SGD itself is probably not the source of nutrients, but rather the pathway by which nutri-

Table 3
Effective freshwater endmember (C^*_{fw}), seawater endmember (C_{sw}), well E average concentrations ($C_{well\ E}$) and estimated fluxes of nutrients associated with fresh and saline SGD. "Absolute" fluxes were derived by multiplying the "specific" fluxes by the seepage face width (200 m as derived from seepage meters—Taniguchi et al., 2003).

	C^*_{fw} (μmol L^{-1})	C_{sw} (μmol L^{-1})	$C_{well\ E}$ (μmol L^{-1})	Specific total SGD fluxes (mmol m^{-2} day^{-1})	Absolute total SGD fluxes mmol m^{-1} day^{-1}	Relative fluxes	
						Fresh SGD (%)	Saline SGD (%)
Summer							
DOC	2596 ± 135	268	383 ± 9	26.9	5382	34	66
Silicate	107 ± 2	11	43.6 ± 3	5.4	1085	7	93
Nitrate	857 ± 127	2	0.2 ± 0.1	3.0	600	100	0
Ammonium	−73 ± 80	1	19.4 ± 2	2.7	535	0	100
DON	301 ± 48	15	21.2 ± 2	2.0	403	52	48
Winter							
DOC	1237 ± 41	323	415 ± 9	18.9	3783	16	84
Silicate	108 ± 2	14	53 ± 1	6.9	1382	4	96
Nitrate	151 ± 34	0	40.1 ± 0.1	0.4	79	95	4
Ammonium	−14 ± 9	0	20.4 ± 1	3.4	682	0	100
DON	44 ± 5	15	19.4 ± 1	0.9	183	12	88

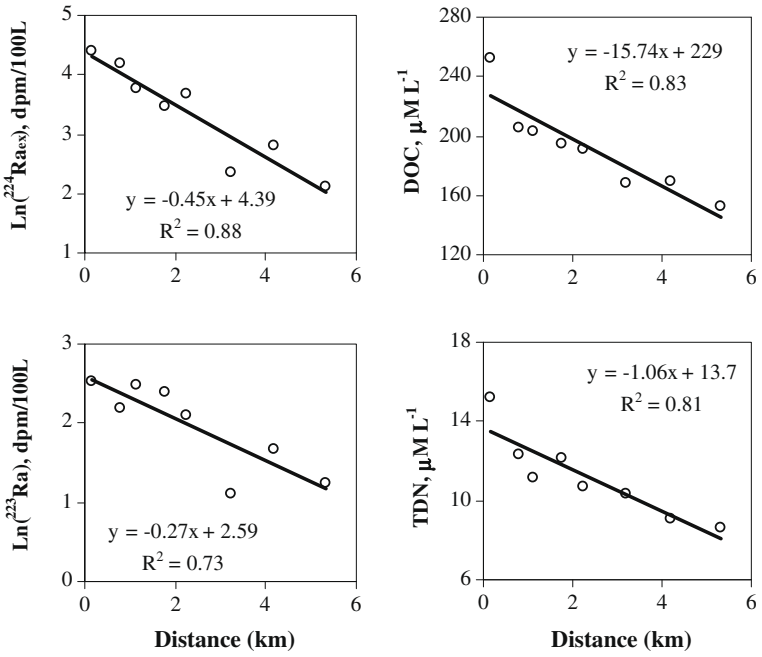

Fig. 10. Offshore transects of ^{224}Ra, ^{223}Ra, DOC, and TDN in seawater sampled in May 2007.

ents produced in the STE are driven into the ocean by the terrestrial hydraulic gradient. We suspect, however, that labile marine organic matter is the ultimate source of the nutrients to the transport mechanisms discussed here (both fresh and saline SGD). Future investigations should determine the source of organic matter, as this may elucidate whether SGD is a source of "new" nutrients to the coastal ocean or purely a recycling mechanism. Stable isotope investigations may help to answer this question.

3.5. Seasonal controls

The groundwater table level, ^{222}Rn-derived total SGD rates, and tidal ranges did not vary seasonally (Table 1), so these factors cannot account for the observed variation in the SGD nutrient fluxes. A major seasonal contrast at this site is the higher summer primary productivity. We suggest that a positive feedback links primary production and SGD nutrient inputs. Visual observations suggest much higher phytoplankton productivity in the summer and seagrass accumulation on the beach. Indeed, nitrogen uptake rates of 300 mg N m^{-2} d^{-1} in the summer and only 17 mg N m^{-2} d^{-1} in the winter occur in the nearby Apalachicola Bay (Mortazavi et al., 2000). We hypothesize that phytoplankton cells driven by tidal pumping into the STE are the source of organic matter that is quickly remineralized at warm temperatures, releasing large amounts of dissolved nutrients. Particulate organic matter accumulation may be greater than remineralization rates when it is cold. Higher microbial activity in warm months would lead to greater rates of nutrient regeneration, explaining higher summertime nutrient production in the STE and SGD of nutrients to coastal waters, stimulating primary production.

This hypothesis is very similar to mechanisms recently advanced for permeable shelf sands. Filtration through permeable shelf sediments promotes the rapid degradation of phytoplankton, making sands a biocatalytic converter for organic matter (Huettel et al., 1996; Rao et al., 2007; Eyre et al., 2008). Studies conducted in the South Atlantic Bight (Jahnke et al., 2005) and in the Delaware Estuary (Ullman et al., 2003) indicated that seasonal changes in groundwater nutrient concentrations were due to variations in sedimentary remineralization rates. If seasonal nutrient regeneration in the STE proves to be a major nutrient source, this could reconcile an apparent paradox observed in nearby Apalachicola Bay. Because riverine nitrogen inputs are one order of magnitude higher in the winter than in the summer (Mortazavi et al., 2000), this is the opposite of what would be predicted if nutrients limit primary production and the Apalachicola River (the largest in Florida) is the major local nutrient source.

3.6. Offshore fluxes from radium isotopes

Nearshore saline SGD as a major source of nutrients to Gulf of Mexico coastal waters is supported by decreasing seawater nutrient concentrations in the offshore direction (Fig. 10). This is further supported by significant correlations ($r > 0.75$; $n = 8$; $p < 0.05$) between nutrients and short-lived radium isotopes, a valuable tracer for the marine component of SGD (Mulligan and Charette, 2006; Peterson et al., 2008). We use the offshore distribution of radium isotopes to estimate offshore nutrient mixing losses. In short, the slope of the natural logarithm plotted against distance from the shore is described as follows (Moore, 2000):

$$m = \sqrt{\frac{\lambda}{K_h}} \tag{5}$$

where m is the slope of the ln-linear curve of the tracer (Fig. 10); λ is the decay constant for ^{224}Ra (0.189 d^{-1}) or ^{223}Ra (0.061 d^{-1}); and K_h is the mixing coefficient ($m^2\ s^{-1}$). We found mixing coefficients of 11.1 and 9.8 $m^2\ s^{-1}$ for ^{224}Ra and ^{223}Ra, respectively. These mixing coefficients were then multiplied by the linear gradient of nutrients versus distance offshore (Fig. 10) and by the average depth of the mixed layer (2 m), providing an offshore nutrient flux along the transect (Moore, 2000; Santos et al., 2008c). The estimated offshore fluxes per unit length of shoreline were 7100 and 480 mmol $m^{-1}\ day^{-1}$ for DOC and TDN, respectively. These values are similar to the absolute SGD nutrient fluxes shown in Table 3, indicating that most of the SGD inputs are transported out of the near-coastal zone. We emphasize, however, that any comparison between SGD and the independently estimated offshore fluxes is hindered by the fact that the offshore transect was performed only during the Vertical TS experiment (May 2007), while SGD fluxes are available only for the Horizontal TS (August 2007 and January 2008) experiments.

3.7. Contrasting surface and subterranean estuaries

After Moore's (1999) benchmark paper coining the term "subterranean estuary", few investigations have compared subterranean and surface estuaries. Because nearby surface estuaries (e.g., Apalachicola and Ochlocknee Rivers) have been investigated in detail before (Kaul and Froelich, 1984; Mortazavi et al., 2000; Mortazavi et al., 2001), comparisons are convenient in our case. We will compare the spatial scale of the mixing processes, water residence times, nitrogen speciation, and dominance of production or consumption.

The spatial scale of the mixing zone is perhaps the most obvious difference. While salinity at this STE ranges from fresh to saline water over just a few meters, surface estuaries typically mix over kilometer scales. Therefore, even though water moves much slower in STE, their smaller spatial scale may lead to similar residence times. For example, the residence time in the upper meter of the STE investigate here was no more than 20 days, while the residence time of the nearby Apalachicola Bay ranged from 5 to 12 days (Dulaiova and Burnett, 2008).

A major contrast relates to nutrient speciation. Our average estimates of SGD-derived nitrogen inputs into the coastal ocean were 7.7 and 4.7 mmol $m^{-2}\ d^{-1}$ in the summer and winter, respectively, consisting of 54% ammonium, 24% nitrate, and 23% DON on average (Table 3). In many surface estuaries and in the coastal ocean, the dissolved N and P pools are dominated by organic rather than inorganic species (Harrison et al., 2005; Dafner et al., 2007). For instance, nitrogen export from the Apalachicola River consists of about 60% DON (Fu and Winchester, 1994). Nitrogen budgets based on only inorganic loading, as done in many previous SGD studies, underestimate bioavailable N loading, whereas total N budgets overestimate bioavailable inputs (Seitzinger et al., 2002). Therefore, the larger contribution of inorganic forms in SGD may facilitate biological uptake.

Regarding the biogeochemical reaction rates, we found that nutrient production dominates in the STE, while removal often dominates in surface estuaries (Kaul and Froelich, 1984; Dafner et al., 2007). DOC mixes conservatively in most surface estuaries (Middelburg and Herman, 2007), in contrast to the production of DOC inferred at the STE investigated here. Excess nutrients in surface estuaries are usually attributed to anthropogenic sources rather than biogeochemical production (Niencheski and Windom, 1994). Therefore, simply multiplying nutrient concentrations from the freshwater endmember by the water discharge will often overestimate nutrient exports to coastal waters from surface estuaries, while the same procedure will underestimate nutrient exports associated with SGD. This demonstrates the importance of determining the effective endmember concentrations (C^*_{fw}) and assessing the biogeochemistry of the mixing zone, as illustrated in Section 3.4.

4. CONCLUSIONS

Our intensive, spatially distributed measurements in shallow beach groundwaters indicated large variability in nutrient concentrations over-time scales ranging from hours to months. The dominant form of nitrogen in this subterranean estuary was DON in the freshwater portion, nitrate in brackish waters, and ammonium in saline waters. Active nutrient cycling in this STE was apparently fueled by oxygen and labile organic matter inputs driven by tidal pumping. Our results point to a complex combination of biogeochemical processes that are likely to occur simultaneously. Oxic remineralization and denitrification probably explain the distribution patterns observed. The STE investigated here is a site of net nutrient regeneration, contrasting to most surface estuaries where nutrient consumption dominates. Nutrient production in the STE for the summer was much higher than in the winter, following a trend similar to coastal primary production. We thus suggest an association between coastal phytoplankton densities and nutrient production in this STE linked to seasonal cycle of labile organic matter accumulation and remineralization in permeable sediments.

Our SGD nutrient flux calculations indicate that even though marine drivers account for ~95% of total SGD volumetric additions, fresh SGD is an important pathway of nutrients as a result of biogeochemical additions across the mixing zone. This pathway accounted for ~25% of DOC and ~50% of total nitrogen inputs, with the remainder associated with a one-dimensional vertical seawater recirculation along a seepage face extending at least 200 m offshore. SGD-derived fluxes in the summer are about 40% higher for DOC and 60% higher for TDN compared to the winter. The common assumption in SGD studies is that endmember nutrient concentrations are relatively constant over time and the groundwater fluxes are variable. However, our results suggest that while SGD volumetric inputs are similar seasonally (Santos, 2008), changes in the biogeochemical conditions of the STE lead to higher nutrient fluxes in the summer. Both SGD volumetric additions and nutrient concentrations in beach groundwater can be highly variable over short-time scales, illustrating the

importance of assessing the biogeochemistry and dynamics of the STE for estimating SGD nutrient fluxes.

ACKNOWLEDGMENTS

This project was sponsored by NSF (OCE05-20723). I Santos hold a Fulbright/CAPES fellowship. Richard Peterson, Natasha Dimova, and Benjamin Mwashote provided valuable help throughout this project. We thank the Florida State University Coastal and Marine Laboratory (FSUCML) personnel for their helpful support and Markus Huettel for kindly allowing us to perform nutrient analysis in his laboratory. The manuscript benefited from thoughtful comments by two anonymous reviewers and the associated editor.

REFERENCES

Addy K., Gold A., Nowicki B., McKenna J., Stolt M. and Groffman P. (2005) Denitrification capacity in a subterranean estuary below Rhode Island fringing salt marsh. *Estuaries* **28**, 896–908.

An S. and Joye S. B. (2001) Enhancement of coupled denitrification by benthic photosynthesis in shallow subtidal estuarine sediments. *Limnology and Oceanography* **43**, 62–74.

Beck A. J., Tsukamoto Y., Tovar-Sanchez A., Huerta-Diaz M., Bokuniewicz H. J. and Sanudo-Wilhelmy S. A. (2007) Importance of geochemical transformations in determining submarine groundwater discharge-derived trace metal and nutrient fluxes. *Applied Geochemistry* **22**, 477–490.

Bianchi T. S., Pennock J. R. and Twilley R. R. (1999) *Biogeochemistry of Gulf of Mexico Estuaries*. John Wiley and Sons, New York.

Boyle E., Collier R., Dengler A. T., Edmond J. M., Ng A. C. and Stallard R. F. (1974) On the chemical mass-balance in estuaries. *Geochimica et Cosmochimica Acta* **38**, 1719–1728.

Boynton W. R., Garber J. H., Summers R. and Kemp W. M. (1995) Inputs, transformations, and transport of nitrogen and phosphorus in Chesapeake Bay and selected tributaries. *Estuaries* **18**, 285–314.

Burnett W., Bokuniewicz H., Huettel M., Moore W. S. and Taniguchi M. (2003) Groundwater and pore water inputs to the coastal zone. *Biogeochemistry* **66**, 3–33.

Burnett W. C., Aggarwal P. K., Aureli A., Bokuniewicz H., Cable J. E., Charette M. A., Kontar E., Krupa S., Kulkarni K. M., Loveless A., Moore W. S., Oberdorfer J. A., Oliveira J., Ozyurt I. N., Povinec P., Privitera A. M. G., Rajar R., Ramessur R. T., Schollten J., Stieglitz T., Taniguchi M. and Turner J. V. (2006) Quantifying submarine groundwater discharge in the coastal zone via multiple methods. *Science of the Total Environment* **367**, 498–543.

Burnett W. C. and Dulaiova H. (2003) Estimating the dynamics of groundwater input into the coastal zone via continuous radon-222 measurements. *Journal of Environmental Radioactivity* **69**, 21–35.

Burnett W. C., Wattayakorn G., Taniguchi M., Dulaiova H., Sojisuporn P., Rungsupa S. and Ishitobi T. (2007) Groundwater-derived nutrient inputs to the Upper Gulf of Thailand. *Continental Shelf Research* **27**, 176–190.

Cable J. E., Burnett W. C., Chanton J. P. and Weatherly G. L. (1996) Estimating groundwater discharge into the northeastern Gulf of Mexico using radon-222. *Earth and Planetary Science Letters* **144**, 591–604.

Cable J. E., Corbett D. and Walsh M. M. (2002) Phosphate uptake in coastal limestone aquifers: a fresh look at wastewater management. *Limnology and Oceanography Bulletin* **11**, 1–4.

Charette M. A. and Allen M. C. (2006) Precision groundwater sampling in coastal aquifers using a direct push shielded-screen well-point system. *Groundwater Monitoring & Remediation* **26**, 87–93.

Charette, M. A. and Sholkovitz, E. R. (2002). Oxidative precipitation of groundwater-derived ferrous iron in the subterranean estuary of a Coastal Bay. *Geophysical Research Letters* **29** (Article No. 1444), doi:10.1029/2001GL014512.

Charette M. A. and Sholkovitz E. R. (2006) Trace element cycling in a subterranean estuary: part 2. Geochemistry of the pore water. *Geochimica et Cosmochimica Acta* **70**, 811–826.

Charette M. A., Splivallo R., Herbold C., Bollinger M. S. and Moore W. S. (2003) Salt marsh submarine groundwater discharge as traced by radium isotopes. *Marine Chemistry* **84**, 113–121.

Dafner E. V., Mallin M. A., Souza J. J., Wells H. A. and Parsons D. C. (2007) Nitrogen and phosphorus species in the coastal and shelf waters of Southeastern North Carolina, Mid-Atlantic U.S. coast. *Marine Chemistry* **103**, 289–303.

Davies P. and Eyre B. D. (2005) Estuarine modification of nutrient and sediment exports to the Great Barrier Reef Marine Park from the Daintree and Annan River catchments. *Marine Pollution Bulletin* **51**, 174–185.

Deborde J., Anschutz P., Auby I., Gle C., Commarieu M.-V., Maurer D., Lecroart P. and Abril G. (2008) Role of tidal pumping on nutrient cycling in a temperate lagoon (Arcachon Bay, France). *Marine Chemistry* **109**, 98–114.

Dulaiova H. and Burnett W. C. (2008) Evaluation of the flushing rates of Apalachicola Bay, Florida via natural geochemical tracers. *Marine Chemistry* **109**, 395–408.

Eyre B. D., Glud R. N. and Patten N. (2008) Mass coral spawning: a natural large-scale nutrient addition experiment. *Limnology and Oceanography* **53**, 997–1013.

Fetter C. W. (2001) *Applied Hydrogeology*. Prentice Hall, Upper Saddle River, NJ.

Fu J.-M. and Winchester J. W. (1994) Sources of nitrogen in three watersheds of northern Florida, USA: mainly atmospheric deposition. *Geochimica et Cosmochimica Acta* **58**, 1581–1590.

Grasshoff K., Ehrhardt M. and Kremling K. (1999) *Methods of Seawater Analysis*. John Wiley & Sons, Weinheim.

Harrison, J. A., Caraco, N. and Seitzinger, S. P. (2005). Global patterns and sources of dissolved organic matter export to the coastal zone: results from a spatially explicit, global model. *Global Biogeochemical Cycles* **19,** GB4S04, doi:10.1029/2005GB002480.

Hays R. L. and Ullman W. J. (2007) Dissolved nutrient fluxes through a sandy estuarine beachface (Cape Henlopen, Delaware, USA): contributions from fresh groundwater discharge, seawater recycling, and diagenesis. *Estuaries and Coasts* **30**, 710–724.

Hu, C., Muller-Karger, F. E. and Swarzenski, P. W. (2006). Hurricanes, submarine groundwater discharge, and Florida's red tides. *Geophysical Research Letters* **33,** L11601, doi:10.1029/2005GL025449.

Huettel M. and Rusch A. (2000) Transport and degradation of phytoplankton in permeable sediment. *Limnology and Oceanography* **45**, 534–549.

Huettel M., Ziebis W. and Forster S. (1996) Flow-induced uptake of particulate matter in permeable sediments. *Limnology and Oceanography* **41**, 309–322.

Jahnke R., Richards M., Nelson J., Robertson C., Rao A. and Jahnke D. (2005) Organic matter remineralization and porewater exchange rates in permeable South Atlantic Bight continental shelf sediments. *Continental Shelf Research* **25**, 1433–1452.

Kaul L. W. and Froelich P. N. (1984) Modeling estuarine nutrient geochemistry in a simple system. *Geochimica et Cosmochimica Acta* **48**, 1417–1433.

Kim, G. and Hwang, D. W. (2002). Tidal pumping of groundwater into the coastal ocean revealed from submarine Rn-222 and CH_4 monitoring. *Geophysical Research Letters* **29,** doi:10.1029/2002GL015093.

Kroeger K. D. and Charette M. A. (2008) Nitrogen biogeochemistry of submarine groundwater discharge. *Limnology and Oceanography* **53**, 1025–1039.

Kroeger K. D., Swarzenski P. W., Greenwood W. J. and Reich C. (2007) Submarine groundwater discharge to Tampa Bay: nutrient fluxes and biogeochemistry of the coastal aquifer. *Marine Chemistry* **104**, 85–97.

Lambert M. and Burnett W. (2003) Submarine groundwater discharge estimates at a Florida coastal site based on continuous radon measurements. *Biogeochemistry* **66**, 55–73.

Martin J. B., Cable J. E., Jaeger J. M., Hartl K. and Smith C. G. (2006) Thermal and chemical evidence for rapid water exchange across the sediment–water interface by bioirrigation in the Indian River Lagoon, Florida. *Limnology and Oceanography* **51**, 1332–1341.

Martin, J. B., Cable, J. E., Smith, C., Roy, M. and Cherrier, J. (2007). Magnitudes of submarine groundwater discharge from marine and terrestrial sources: Indian River Lagoon, Florida. *Water Resources Research* **43,** W05440, doi:10.1029/2006WR005266.

Middelburg J. J. and Herman P. M. J. (2007) Organic matter processing in tidal estuaries. *Marine Chemistry* **106**, 127–147.

Moore W. S. (1999) The subterranean estuary: a reaction zone of groundwater and seawater. *Marine Chemistry* **65**, 111–126.

Moore W. S. (2000) Determining coastal mixing rates using radium isotopes. *Continental Shelf Research* **20**, 1993–2007.

Moore W. S. and Arnold R. (1996) Measurement of ^{223}Ra and ^{224}Ra in coastal waters using a delayed coincidence counter. *Journal of Geophysical Research* **101**, 1321–1329.

Mortazavi B., Iverson R. L. and Huang W. (2001) Dissolved organic nitrogen and nitrate in Apalachicola Bay, Florida: spatial distributions and monthly budgets. *Marine Ecology Progress Series* **214**, 79–91.

Mortazavi B., Iverson R. L., Huang W., Lewis F. G. and Caffrey J. M. (2000) Nitrogen budget for Apalachicola Bay, a bar built estuary in the northeastern Gulf of Mexico. *Marine Ecology Progress Series* **195**, 1–14.

Mulligan A. E. and Charette M. A. (2006) Intercomparison of submarine groundwater discharge estimates from a sandy unconfined aquifer. *Journal of Hydrology* **327**, 411–425.

Niencheski L. F. and Windom H. L. (1994) Nutrient flux and budget in Patos Lagoon estuary. *The Science of the Total Environment* **149**, 53–60.

Paytan A., Shellenbarger G. G., Street H. J., Gonneea E. M., Davis K. A., Young B. M. and Moore W. S. (2006) Submarine groundwater discharge: an important source of new inorganic nitrogen to coral reef ecosystems. *Limnology and Oceanography* **51**, 343–348.

Peterson, R. N., Burnett, W. C., Taniguchi, M., Chen, J., Santos, I. R. and Ishitobi, T. (2008). Radon and radium isotope assessment of submarine groundwater discharge in the Yellow River Delta, China. *Journal of Geophysical Research* **113,** C09021, doi:10.1029/2008JC004776.

Pinckney J. L., Paerl H. W., Tester P. and Richardson T. L. (2001) The role of nutrient loading and eutrophication in estuarine ecology. *Environmental Health Perspectives* **109**, 699–706.

Rao A. M. F., McCarthy M. J., Gardner W. S. and Jahnke R. A. (2007) Respiration and denitrification in permeable continental shelf deposits on the South Atlantic Bight: rates of carbon and nitrogen cycling from sediment column experiments. *Continental Shelf Research* **27**, 1801–1819.

Robinson C., Li L. and Barry D. A. (2007) Effect of tidal forcing on a subterranean estuary. *Advances in Water Resources* **30**, 851–865.

Rouxel O., Sholkovitz E., Charette M. and Edwards K. J. (2008) Iron isotope fractionation in subterranean estuaries. *Geochimica et Cosmochimica Acta* **72**, 3413–3430.

Santos I. R., Burnett W., Chanton J. P., Mwashote B., Suryaputra I. G. N. A. and Dittmar T. (2008a) Nutrient biogeochemistry in a Gulf of Mexico subterranean estuary and groundwater-derived fluxes to the coastal ocean. *Limnology and Oceanography* **53**, 705–718.

Santos I. R., Machado M. I., Niencheski L. F., Burnett W., Milani I. B., Andrade C. F. F., Peterson R. N., Chanton J. and Baisch P. (2008b) Major ion chemistry in a freshwater coastal lagoon from southern Brazil (Mangueira Lagoon): influence of groundwater inputs. *Aquatic Geochemistry* **14**, 133–146. doi:10.1007/s10498-008-9029-0.

Santos I. R., Niencheski F., Burnett W., Peterson R., Chanton J. P., Andrade C. F. F., Milani I. B., Schmidt A. and Knoeller K. (2008c) Tracing anthropogenically driven groundwater discharge into a coastal lagoon from southern Brazil. *Journal of Hydrology* **353**, 275–293. doi:10.1016/j.jhydrol.2008.02.010.

Santos I.R. (2008). *Submarine groundwater discharge driving mechanisms and biogeochemical aspects.* PhD Dissertation, Department of Oceanography, Florida State University.

Seitzinger, S. P., Harrison, J. A., Dumont, E., Beusen, A. H. W. and Bouwman, A. F. (2005). Sources and delivery of carbon, nitrogen, and phosphorus to the coastal zone: an overview of Global Nutrient Export from Watersheds (NEWS) models and their application. *Global Biogeochemical Cycles* **19,** GB4S01, doi:10.1029/2005GB002606.

Seitzinger S. P., Sanders R. W. and Styles R. V. (2002) Bioavailability of DON from natural and anthropogenic sources to estuarine plankton. *Limnology and Oceanography* **47**, 353–366.

Slomp C. P. and Van Cappellen P. (2004) Nutrient inputs to the coastal ocean through submarine groundwater discharge: controls and potential impact. *Journal of Hydrology* **295**, 64–86.

Smith L. and Zawadzki W. (2003) A hydrogeologic model of submarine groundwater discharge: Florida intercomparison experiment. *Biogeochemistry* **66**, 95–110.

Spiteri C., Slomp C. P., Charette M. A., Tuncay K. and Meile C. (2008) Flow and nutrient dynamics in a subterranean estuary (Waquoit Bay, MA, USA): field data and reactive transport modeling. *Geochimica et Cosmochimica Acta* **72**, 3398–3412.

Taniguchi M., Burnett W., Smith C., Paulsen R., O'Rourke D., Krupa S. and Christoff J. (2003) Spatial and temporal distributions of submarine groundwater discharge rates obtained from various types of seepage meters at a site in the Northeastern Gulf of Mexico. *Biogeochemistry* **66**, 35–53.

Taniguchi M. and Iwakawa H. (2004) Submarine groundwater discharge in Osaka Bay, Japan. *Limnology* **5**, 25–32.

Uchiyama Y., Nadaoka K., Rolke P., Adachi K. and Yagi H. (2000) Submarine groundwater discharge into the sea and associated nutrient transport in a sandy beach. *Water Resources Research* **36**, 1467–1479.

Ullman W. J., Chang B., Miller D. C. and Madsen J. A. (2003) Groundwater mixing, nutrient diagenesis, and discharges across a sandy beachface, Cape Henlopen, Delaware (USA). *Estuarine, Coastal and Shelf Science* **57**, 539–552.

Valiela I., Bowen J. L. and Kroeger K. D. (2002) Assessment of models for estimation of land-derived nitrogen loads to estuaries. *Applied Geochemistry* **19**, 935–953.

Windom H. and Niencheski F. (2003) Biogeochemical processes in a freshwater–seawater mixing zone in permeable sediments along the coast of Southern Brazil. *Marine Chemistry* **83**, 121–130.

Windom H. L., Niencheski L. F. and Smith J. R. G. (1999) Biogeochemistry of nutrients and trace metals in the estuarine region of the Patos Lagoon (Brazil). *Estuarine, Coastal and Shelf Science* **48**, 113–123.

Associate editor: Thomas S. Bianchi